AN EXACT SOLUTION FOR THE ASSESSMENT OF NONEQUILIBRIUM SORPTION OF RADIONUCLIDES IN THE VADOSE ZONE

Ronald L. Drake and Jin-Song Chen
Dynamac Corporation
3601 Oakridge Boulevard, Ada, OK 74820

David G. Jewett
U.S. EPA, Office of Research and Development
National Risk Management Research Laboratory
Subsurface Protection and Remediation Division
P.O. Box, 1198, Ada, OK 74820

ABSTRACT

In a report on model evaluation, the authors ran the HYDRUS Code, among other transport codes, to evaluate the impacts of nonequilibrium sorption sites on the time-evolution of ^{99}Tc and ^{90}Sr through the vadose zone. Since our evaluation was based on a rather low, annual recharge rate, many of the numerical results derived from HYDRUS indicated that the nonequilibrium sorption sites, in essence, acted as equilibrium sorption sites. To help explain these results, we considered a "stripped-down" version of the HYDRUS system. This "stripped-down" version possesses two dependent variables, one for the radionuclides in solution and the other for the radionuclides adsorbed to the nonequilibrium sites; and it possesses constant physical parameters. The resultant governing equation for the radionuclides in solution is a linear, advection-dispersion-reaction (i.e., radioactive decay) partial differential equation containing a history integral term accounting for the nonequilibrium sorption sites. It is this "stripped-down" version, which is the subject of this paper. We found an exact solution to this new version of the model. The exact solution is given in terms of a single definite integral of terms involving elementary functions of the independent variables and the system parameters. This integral possesses adequate convergence properties and is easy to evaluate, both in a quantitative matter and in a qualitative manner. The parameters that are considered in the system are as follows: the radionuclide's equilibrium partition coefficient between water and soil, the bulk density of the soil, the fractions of equilibrium/nonequilibrium sorption sites, the volumetric water content, the first order equilibrium adsorption rate constant, the first order radioactive decay rate constant, the liquid water soil tortuosity factor, the molecular diffusion coefficient in water, the longitudinal dispersivity factor, and the Darcian fluid flux density. In addition, the system possesses a stepwise, variable source of radionuclides at the ground surface and a variable flux of pollutants from the vadose zone at the water table. Although this new system is a "stripped down" version of the HYDRUS Code, it is a valuable system in its own right for the assessment of nonequilibrium sorption of radionuclides in the vadose zone.

INTRODUCTION

Knox, et al. (1) and Thibodeaux (2) describe in detail the various processes influencing solid-liquid soil reactions, including those processes characterized as adsorption/desorption. Depending upon the soil structure and texture, the characteristics of the contaminants, and the flow characteristics, the characteristic time scales for physical adsorption/desorption are known to vary from microseconds to months. In addition, experimental evidence has indicated that the solid-phase fraction of a contaminant on the desorption cycle often behaves much different than when the contaminant is on the adsorption cycle. This leads to nonequilibrium soil reaction states and hysteretic type adsorption/desorption cycles. Knox, et al. (1) say that such hysteretic cycles affect the amount of water required in pump and treat remediation of subsurface aquifers. This conclusion is reinforced by the work of Brogan and Gailey (3). These latter authors found that when significant rate limitations to solute transport are present, predictions based on the local equilibrium assumption (LEA) will underestimate the actual cleanup time for pump and treat operations. The slower the mass transfer rates, the longer it will take to achieve desired remedial goals. Conversely, they state that when rate limitations do not appear significant, predictions based on LEA may be appropriate.

Thibodeaux (2) states that the validity of the LEA in solid-liquid soil reactions depends on the degree of interaction between the macroscopic transport processes of water flow and hydrodynamic dispersion, and the microscopic processes of molecular diffusion and sorbed-solute distribution in conjunction with soil aggregate size. When the rate of change of solute mass during macroscopic sorption processes is fast relative to bulk flow, the interaction is nearly instantaneous (comparatively speaking), and it conforms to the LEA. Deviations from local equilibrium occur as the interactions of the solute with the porous media become increasingly time dependent with respect to the time scales of the bulk flow. This divergence also occurs as soil aggregates increase in size and the pore-class heterogeneity increases.

The current authors were exposed to those temporal scaling problems of solid-phase soil reactions while evaluating several numerical, mathematical models of water and chemical movement in soils that could be used as decision aids for determining soil screening levels of radionuclides in the unsaturated, or vadose zone (4). Many of these flow/transport codes require extensive sets of input parameters, and some of the parameters possess high degrees of uncertainty due to soil variability and unknown future meteorological conditions. The impacts of uncertain model parameters upon pertinent model outputs are required for sound modeling applications. Model users need an understanding of these impacts so they can collect the appropriate data for parameter evaluation at a given site and incorporate the uncertainties of model prediction into the decision making process. Of the several models considered in our evaluation of these matters, one model, the HYDRUS Code of the U.S. Salinity Laboratory in Riverside, California (5), has the facility for tracking both the time-evolution of radionuclides in solution and radionuclides at nonequilibrium sites throughout the soil column. The formulation of the equilibrium/nonequilibrium processes in this code is based on the two-site model of van Genuchten and Wagenet (6).

In Chen et al (4), the model calculations and evaluations were conducted at a hypothetical, radionuclide disposal facility using real soil properties and climatic data from a site in

southwestern United States. The transport of radionuclides through this semi-arid, unsaturated zone was under the influence of a very low annual recharge rate, which led to a hydrodynamic dispersion of only three times that of molecular diffusion. Under these conditions, sorption sites that are in local equilibrium at higher recharge rates will still be in local equilibrium. Some new sites where nonequilibrium conditions exist or sites where no liquid-solid reactions occur at higher rates will now become sites governed by LEA under these low flow rates. Other new sites will pass from no action sites under higher flows to nonequilibrium sorption sites under the low flows, and some sites will be nonequilibrium sites under both the higher and lower flows. Thus, the adsorption-desorption cycle of a given pollutant through a given soil profile may exhibit a variety of characteristic time scales dependent upon the types of liquid-solid reaction mechanisms occurring at the various sites in the soil matrix and the flow regimes under which the contaminant moves. Therefore, the current authors thought it was reasonable to consider the occurrence of equilibrium/nonequilibrium sorption sites under all flow regimes, even the low annual recharge rates considered in Chen, et al. (4).

To evaluate the consequences of nonequilibrium sorption sites on the time-evolution of ^{99}Tc and ^{90}Sr migrating through a **finite depth vadose zone**, Chen, et al (4) used the HYDRUS Code. For the low annual recharge rate mentioned above, the HYDRUS numerical results for what was thought to be reasonable choices of the system parameters indicated that the nonequilibrium sorption sites, in essence, acted as equilibrium sorption sites. Parameter sets were found that did exhibit non-Gaussian like behavior (i.e., nonequilibrium behavior) for pollution concentration breakthrough curves (BTCs), but some of the parameters in these sets may have been physically unrealistic. To help explain these results, we considered a "stripped-down" version of the HYDRUS system. This "stripped down" version possesses two dependent variables, one for the radionuclides in solution and the other for the radionuclides adsorbed to the nonequilibrium sites. The two systems possess constant physical parameters. These two systems can be combined to give a resultant governing equation for the radionuclides in solution. This resultant equation is a linear, advection-dispersion-reaction (i.e., radioactive decay) partial integro-differential equation containing a **history integral term** accounting for the nonequilibrium sorption sites. It is this "stripped down" version of HYDRUS, which is the subject of the current paper. In passing, we should note that Toride, et al. (7) have also derived analytical, exact solutions for a similar system. However, Toride, et al., (7) considered **semi-infinite soil systems**, while we consider **finite depth systems**. In addition, several of our solution steps are quite different than those of Toride, et al., (7) and these steps have application to other linear, advection-dispersion-reaction systems.

THE GOVERNING EQUATIONS

For discussion and argument purposes in the report by Chen, et al. (4), the HYDRUS transport equations for the liquid phase pollutant concentration C*, in units of M/L^3, and the nonequilibrium solid phase concentration S*, in units of M/M were simplified as follows:

$$C^*_{,t} + QC^*_{,z} = DC^*_{,zz} - \mu^* C^* - (D/P)\Lambda , \qquad \text{(Eq. 1)}$$

$$S^*_{,t} = (D/P) - \mu^* S^*, \qquad \text{(Eq. 2)}$$

where the subscript comma followed by t or z indicates partial differentiation with respect to t or z, respectively. A letter repeated twice indicates a second partial derivative. The parameters in Equations 1 and 2 are the effective velocity of the sorbing radionuclide through the vadose zone (Q in units of L/T), the effective dispersion coefficient of the sorbing radionuclide in the vadose zone (D in units of L^2/T), the effective bulk density of the porous medium (Λ in units of M/L^3), the first order rate constant for radioactive decay (μ^* in units of 1/T), and a decay/production term (D/P in units of 1/T). The quantities D, (D/P), Q and Λ are defined by:

$$D = \left(\theta\tau_w D_w + D_L q\right) \div R \,, \qquad \text{(Eq. 3)}$$

$$\left(D/P\right) = \omega^*\left[\left(1-f\right) K_d C^* - S^*\right] \,, \qquad \text{(Eq. 4)}$$

$$Q = q \div R, \qquad \Lambda = \rho \div R \,, \qquad \text{(Eq. 5)}$$

where R is a retardation factor defined by

$$R = \theta + \rho\, f\, K_d \,. \qquad \text{(Eq. 6)}$$

The other parameters in Equations 3 to 6 are defined in the following list:

θ	=	volumetric water content, L^3/L^3, or unitless,
τ_w	=	tortuosity factor in the liquid phase, unitless,
D_w	=	molecular diffusion coefficient of the radionuclide in water, L^2/T,
D_L	=	longitudinal dispersivity of the radionuclide, L,
q	=	Darcian fluid flux density of the water, L/T,
ω^*	=	First order adsorption rate constant, 1/T,
f	=	fraction of sorption sites at equilibrium, unitless,
1-f	=	fraction of sorption sites at nonequilibrium, unitless,
K_d	=	distribution coefficient between liquid and solid phases, L^3/M,
ρ	=	bulk density of the porous medium M/L^3.

The initial and boundary conditions corresponding to the transport Equations 1 and 2 are defined over an infinite time interval $t \geq 0$, and a finite depth, vadose zone, where z = 0 at the surface of the zone and z = L at the water table. These conditions are as follows:

$$C^*(z,0) = 0, \quad 0 < z < L \,, \qquad \text{(Eq. 7)}$$

$$S^*(z,0) = 0 \,, \quad 0 < z < L \,, \qquad \text{(Eq. 8)}$$

$$C^*(0,t) = C_0 = \text{Constant} \,, \quad t > 0 \,, \qquad \text{(Eq. 9)}$$

$$C^*_{,z}(L,t) = v_d^* = \text{Constant} \,, \quad t > 0 \,. \qquad \text{(Eq. 10)}$$

Equation 9 represents a constant surface source of radionuclides such that the concentration in the recharge water is C_0, while Equation 10 fixes the concentration gradient at the water table at v_d^* in M/L^4 units.

Nonequilibrium Sorption Site Input Parameters

The nonequilibrium sorption process in Equations 1 to 10 is defined by the two input parameters (f,ω^*). When $f = 1$, there are no nonequilibrium sorption sites in the soil column, $0 \leq z \leq L$; when $f = 0$, there are no equilibrium sorption sites in the column. When $0 < f < 1$, there are both equilibrium and nonequilibrium sites. The quantity ω^* is the first order rate constant for nonequilibrium sorption and plays a key role in the decay/production term (D/P), in Equations 1 and 2.

To assess the effects of ω^* and (D/P) on the C* and S* distributions, Chen, et al. (4) let the initial distribution of C* and S* in the soil column be zero and postulated a constant source of contaminant at the surface ($z = 0$), see Equations 7 to 9. For a contaminant whose half-life is much greater than its passage through the soil column (e.g., ^{99}Tc), the effect of μ^* in Equations 1 and 2 on the BTCs at the water table is greatly over shadowed by the decay/production term (D/P). As the contamination process begins ($t > 0$), pollutant C* begins to spread throughout the water in the soil column. This spreading of C* then produces a source of S* in the profile via the (D/P) term. Thus, S* begins to spread throughout the soil matrix in the vertical column. As long as S* is less than $(1 - f)\, K_d C^*$, (D/P) is a sink term for C* and a source for S*. If $S^* > (1 - f)\, K_d C^*$, then (D/P) is a source for C* and a sink term for S*. Since the only other term in the S* equation is the very small term $\mu^* S^*$ (assumed to be small at the moment, such as that for ^{99}Tc), S* will rapidly approach the "equilibrium" condition for sufficiently large ω^*:

$$S^* \cong (1 - f)\, K_d C^*. \qquad \text{(Eq. 11)}$$

As S* approaches the "equilibrium" condition, (D/P) turns off in the C* and S* equations. If C* and S* do not become out of balance again, as defined by Equation 11, the nonequilibrium sorption process acts as an equilibrium sorption process as was evident in several cases analyzed by Chen, et al. (4). Further, Equation 11 shows that for low K_d-pollutants (e.g., ^{99}Tc), the amount of material adsorbed at the nonequilibrium sites at any given time is very small; while for high K_d-pollutants (e.g., ^{99}Ru), the opposite is usually true. Hence, for maximum nonequilibrium sorption site effects, f should be small relative to unity, ω^* should be sufficiently small, μ^* should be sufficiently large relative to the pollutant's passage through the soil column, and K_d should be larger than unity. For minimal nonequilibrium sorption site effects, f should be close to unity, ω^* should be sufficiently large, μ^* should be sufficiently small, and K_d should be much smaller than unity. The specific degrees of largeness and smallness for these various parameters can be determined by analyzing the exact solution of Equations 1 to 10, to which we now turn.

Nondimensional Form of the Governing Equations

The characteristic length and time are taken to be L and L^2/D, respectively, while the characteristic concentration is taken as C_0. Thus, the nondimensional variables and parameters are given by:

$$x = z/L,\ 0 \le x \le 1;\ \tau = tD/L^2,\ \tau > 0, \qquad \text{(Eq. 12)}$$

$$C = C(x,\tau) = C^*(z,t) \div C_0;\quad S = S(x,\tau) = S^*(z,t)\ , \qquad \text{(Eq. 13)}$$

$$\mu = \mu^* L^2/D\ ;\quad \omega = \omega^* L^2/D\ , \qquad \text{(Eq. 14)}$$

where μ and ω are macroscopic Sherwood Numbers which are ratios of mass diffusivities (due to decay and phase transfer, respectively) to dispersive diffusivity (8). Combining Equations 12 to 14 with Equations 1, 2, and 7 to 10 results in the following nondimensional system:

$$C_{,\tau} + 2BC_{,x} = C_{,xx} - \mu C - \omega\Lambda(1-f)\,K_d C + \omega\Lambda S/C_0\ , \qquad \text{(Eq. 15)}$$

$$S_{,t} + (\mu+\omega)\,S = \omega(1-f)\,K_d C_0 C\ , \qquad \text{(Eq. 16)}$$

$$C(x,0) = 0,\ 0 < x < 1\ , \qquad \text{(Eq. 17)}$$

$$S(x,0) = 0,\ 0 < x < 1\ , \qquad \text{(Eq. 18)}$$

$$C(0,\tau) = 1,\ \tau > 0\ , \qquad \text{(Eq. 19)}$$

$$C_{,x}(1,\tau) = v_d^*\, L/C_0 = v_d,\ \tau > 0\ , \qquad \text{(Eq. 20)}$$

where B is a mass transfer Peclet Number which is a ratio of bulk mass transfer to dispersive mass transfer (8):

$$B = \frac{LQ}{2D}\ . \qquad \text{(Eq. 21)}$$

TRANSFORMATION OF THE (C,S)-SYSTEM

The next step in the solution process of Equations 15 to 20 is a series of transformations: the elimination of S in Equation 15, the elimination of the $2BC_{,x}$ term in Equation 15, and the Laplace transform of the resulting C-system.

Elimination of S(x,τ)

The solution of Equations 16 and 18 for S in terms of C is given by

$$\begin{aligned} S(x,\tau) &= \omega(1-f)\,K_d C_0 \int_0^\tau \exp\left[-(\mu+\omega)(\tau-\eta)\right] C(x,\eta)\,d\eta\ , \\ &= \left[\omega(1-f)\,K_d C_0\right] \exp\left[-(\mu+\omega)\tau\right] * C(x,\tau)\ , \end{aligned} \qquad \text{(Eq. 22)}$$

where "*" indicates the convolution of two functions with respect to nondimensional time τ. Substituting Equation 22 into Equation 15 results in the following:

$$C_{,\tau} + 2BC_{,x} = C_{,xx} - \left[b - B^2 + \mu + \omega\right] C - a \exp\left[-(\mu + \omega)\tau\right] * C \,, \qquad \text{(Eq. 23)}$$

where a and b are defined by

$$a = -\omega^2 \, (1 - f) \, \Lambda K_d \leq 0 \,, \qquad \text{(Eq. 24)}$$

$$b = B^2 - \omega + \omega \, \Lambda (1 - f) \, K_d \,. \qquad \text{(Eq. 25)}$$

Elimination of $2BC_{,x}$

The $2BC_{,x}$ term in Equation 23 can be eliminated by invoking the following substitution:

$$E(x,\tau) = \exp\left[-Bx\right] C(x,\tau) \,. \qquad \text{(Eq. 26)}$$

Substituting Equation 26 into Equations 17, 19, 20, and 23 defines the governing equations for $E(x,\tau)$:

$$E_{,\tau} - E_{,xx} + \left[b + \mu + \omega\right] E + a \exp\left[-(\mu + \omega)\tau\right] * E = 0 \,, \qquad \text{(Eq. 27)}$$

$$E(x,0) = 0 \,, \quad 0 < x < 1 \,, \qquad \text{(Eq. 28)}$$

$$E(0, \tau) = 1 \,, \quad \tau > 0 \,, \qquad \text{(Eq. 29)}$$

$$B \, E(1,\tau) + E_{,x}(1,\tau) = V, \; \tau > 0 \,, \qquad \text{(Eq. 30)}$$

where $V = \exp(-B) \, v_d = \exp(-B) \, v_d * L/C_0 \leq 0$.

Laplace Transform of the E-System

The Laplace transform of any admissible function $F(x,\tau)$ is defined by Debnath (9) and Duffy (10):

$$\bar{F}(x,s) = L\left[F(x,\tau)\right] = \int_0^\infty \exp\left[-s\tau\right] F(x,\tau) \, d\tau \,. \qquad \text{(Eq. 31)}$$

Applying this operation to Equations 27 to 30 results in the following transformed system:

$$\bar{E}''(x,s) - G^2(s) \, E(x,s) = 0 \,, \qquad \text{(Eq. 32)}$$

$$\bar{E}\,(0,s) = 1/s \,, \qquad \text{(Eq. 33)}$$

$$B \, \bar{E}(1,s) + \bar{E}'(1,s) = V/s \,, \qquad \text{(Eq. 34)}$$

where " ′ " and " ″ " indicate first and second derivatives, respectively, with respect to x, and G(s) is defined by:

$$G(s) = \left[s + \mu + \omega + \frac{a}{s+\mu+\omega} + b \right]^{1/2} . \qquad \text{(Eq. 35)}$$

SOLUTION OF THE TRANSFORMED E-SYSTEM

The general solution of Equations 32 to 35 is given by

$$\bar{E}(x,s) = A(s) \sinh\left[(1-x)\, G(s)\right] + B(s) \cosh\left[(1-x)\, G(s)\right] , \qquad \text{(Eq. 36)}$$

where A(s) and B(s) are determined from Equations 33 and 34. Deriving A(s) and B(s) results in the following solution for the $\bar{E}-$system:

$$\bar{E}(x,s) = \left[\frac{\left\{B - V \cosh\left[G(s)\right]\right\} \sinh\left[(1-x)\, G(s)\right]}{B \sinh\left[G(s)\right] + G(s)\cosh\left[G(s)\right]} + \frac{\left\{G(s) + V \sinh\left[G(s)\right]\right\} \cosh\left[(1-x)\, G(s)\right]}{B \sinh\left[G(s)\right] + G(s)\cosh\left[G(s)\right]} \right] \frac{1}{s} . \qquad \text{(Eq. 37)}$$

Tauberian Theorems

Applying the Tauberian Theorems (9) allows the behavior of $E(x,\tau)$ to be determined from the transformed function $\bar{E}(x,s)$ if the limit of $\bar{E}(x,s)$ as $s \to \infty$ is zero. This limiting condition is satisfied since for large s, $\bar{E}(x,s)$ is approximately equal to $s^{-1} \exp[-x\, G(s)]$ which approaches zero for all x, $0 \le x \le 1$, as $s \to \infty$. The first Tauberian theorem is the **Initial Value Theorem**:

$$\begin{aligned} \lim_{s\to\infty} \left[s\, \bar{E}(x,s) \right] &= \lim_{\tau\to 0} E(x,\tau) = E(x,0) , \\ &= \lim_{s\to\infty} \left\{ \exp\left[-x\, G(s)\right] \right\} = 0, \quad 0 < x \le 1 , \end{aligned} \qquad \text{(Eq. 38)}$$

which satisfies Equation 28.

For abbreviation purposes, let us consider the following:

$$W\left[x,\, G(s)\right] = s\, \bar{E}(x,s) , \qquad \text{(Eq. 39)}$$

$$G = G(0) = \left[\mu + \omega + \frac{a}{\mu+\omega} + b \right]^{1/2} , \qquad \text{(Eq. 40)}$$

where G^2 can be shown to be positive, and thus, G is taken as positive. The second Tauberian Theorem is a **Final Value Theorem**:

$$\int_0^\infty E(x,\tau)\, d\tau = \lim_{s\to 0} \bar{E}(x,s) = W(x,G) \lim_{s\to 0} \frac{1}{s} = \infty , \qquad \text{(Eq. 41)}$$

since W(x,G) is finite and nonzero. This result is reasonable since Equation 29 gives a continuous and uniform source at the surface; hence, an infinite amount of material passes through the soil column in infinite time. The third Tauberian theorem is another **Final Value Theorem**:

$$\lim_{s\to 0} s\bar{E}(x,s) = \lim_{s\to 0} W\left[x,G(s)\right] = \lim_{\tau\to\infty} E(x,\tau) = E(x) = W(x,G) , \qquad \text{(Eq. 42)}$$

where E(x) is the **steady state solution** of the E-system in Equations 27 to 30, and this solution is equal to W(x,G).

INVERSE LAPLACE TRANSFORM OF $\bar{E}(x,s)$

For an expression as complex as the formula for $\bar{E}(x,s)$ in Equation 37, the use of inverse Laplace transform tables, even a set of tables as extensive as those of Oberhettinger and Badii (11), is not very profitable. A much better approach is to use the Bromwich integral

$$E(x,\tau) = \frac{1}{2\pi i} \int_{c-\infty i}^{c+\infty i} \bar{E}(x,s) \exp\left[s\tau\right] ds , \qquad \text{(Eq. 43)}$$

and contour integration in the complex s-plane.

Location of the Singular Points of $\bar{E}(x,s)$

Considering Equations 35 and 37, we note that the radical G(s) produces **no branch points** since G(s) can be factored out of the numerator and denominator in Equation 37, leaving quotients of power series in terms of $G^2(s)$. The expression $\bar{E}(x,s)$ has a **simple pole** at s = 0. Since the term $(s + \mu + \omega)^{-1}$ occurs in all integer powers in the above power series in $G^2(s)$, $s = -(\mu + \omega)$ is an **essential singular point**.

The final set of singular points of $\bar{E}(x,s)$ are obtained from

$$B \sinh\left[G(s)\right] + G(s) \cosh\left[G(s)\right] = 0 . \qquad \text{(Eq. 44)}$$

To find out where the roots of Equation 44 lie in the complex s-plane, let $G(s) = i\alpha_n$, $\alpha_n > 0$. Thus, Equation 44 reduces to the real transcendental equation $\tan(\alpha_n) = -\alpha_n/B$. The roots of this

equation can be obtained by a rapidly converging iterative process, and α_n converges to $(2n-1)\pi/2$, from the right, as $n \rightarrow \infty$. The values of the corresponding singular points s_n in the s-plane are obtained from

$$G^2(s_n) = (s_n + \mu + \omega) - \frac{a}{s_n + \mu + \omega} + b = -\alpha_n^2 \; ; \qquad \text{(Eq. 45)}$$

or solving for s_n, we have:

$$s_n = -(\mu + \omega) - \beta_n \pm \beta_n \left[1 + \frac{|a|}{\beta_n^2}\right]^{1/2} , \qquad \text{(Eq. 46)}$$

where $\beta_n = \left(b + \alpha_n^2\right) \div 2$. The roots s_n, n = 1,2,3, …, for the "-" sign in Equation 46 are more-or-less equally spaced roots (i.e., **simple poles**) along the negative real s-axis to the left of $s = -(\mu + \omega)$. The roots s_n, n = 1,2,3, …, for the "+" sign in Equation (46) can be shown to be negative for all n and to the right of $s = -(\mu + \omega)$ on the real s-axis. Further, as $n \rightarrow \infty$, the s_n to the right of $s = -(\mu + \omega)$ approach $s = -(\mu + \omega)$ in the limit. Thus, $s = -(\mu + \omega)$ is a very complex singular point, namely a **nonisolated, essential singular point**. Except for the simple pole at s = 0, all the singular points of $\bar{E}(x,s)$ are along the negative real axis in the complex s-plane. This is good since the Bromwich integral can be formulated in such a manner as to evade these singular points, especially the complex singular point at $s = -(\mu + \omega)$.

Bromwich's Integral for E(x,τ)

The contour in the Bromwich integral in Equation 43, c - ∞i to c -i∞, c > 0, can be replaced by a contour along the imaginary axis, as shown in Figure 1, since there are no singular points of $\bar{E}(x,s)$ in the right-half s-plane. The integration variable s along with the new contour is replaced by the following substitutions (10):

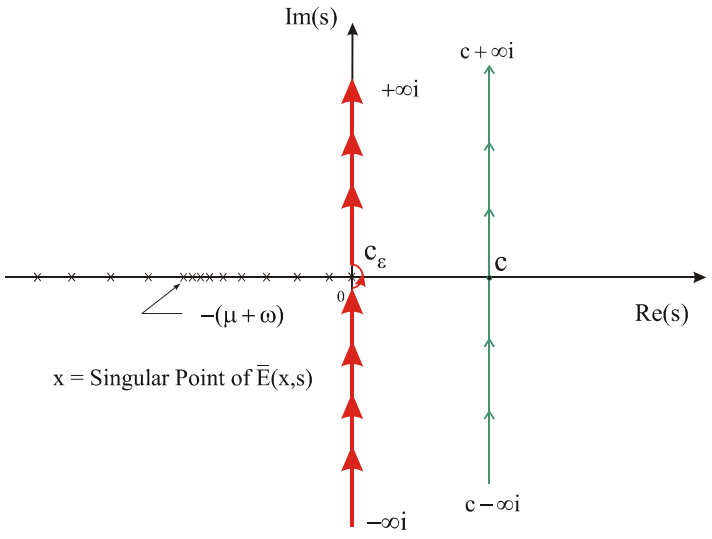

Fig. 1. The contour for the Bromwich integral of the inversion of $\bar{E}(x,s)$.

$$
\begin{aligned}
&-\infty i \rightarrow -0i:\ s = \eta^2/2 \exp\left[-i\,\pi/2\right],\ ds = \eta \exp\left[-i\,\pi/2\right] d\eta,\ 0 < \eta < \infty\ , \\
&\text{half-circle } c_\varepsilon:\ s = \varepsilon \exp[i\theta],\ ds = i\varepsilon \exp[i\theta]\, d\theta,\ -\pi/2 < \theta < \pi/2,\ \varepsilon \rightarrow 0\ , \qquad \text{(Eq. 47)} \\
&+0i \rightarrow +\infty i:\ s = \eta^2/2 \exp\left[i\,\pi/2\right],\ ds = \eta \exp\left[i\,\pi/2\right] d\eta,\ 0 < \eta < \infty\ .
\end{aligned}
$$

In the evaluation of the three segments of the contour integral for $E(x,\tau)$, the integrand $\bar{E}(x,s)\exp(s,\tau)$ must be expressed in terms of real and imaginary parts, each being a function of (x,τ,η) and the system parameters. Considering $\bar{E}(x,s)$ in Equation 37, one sees that the process starts with the radical term G(s). First, the values of $s = \pm i\,\eta^2/2$ are substituted into G(s), giving the following:

$$G\left(\pm i\eta^2/2\right) = \left[C(\eta) \pm iD(\eta)\right]^{1/2} = H(\eta) \pm iF(\eta)\ , \qquad \text{(Eq. 48)}$$

where $C(\eta)$, $D(\eta)$, $H(\eta)$, and $F(\eta)$ will be defined later. The next step is to express the hyperbolic functions of G(s) in terms of real and imaginary parts. Then, the products in the numerators of $\bar{E}(x,s)$ are expressed in real and imaginary parts; after that, the numerator in $\bar{E}(x,s)$ is expressed in real and imaginary parts. Finally, the expression for $\bar{E}(x,s) \bullet \exp[\tau s]$ is expressed in real and imaginary parts; the imaginary parts cancel out, while the real parts contribute to the integral. The contribution from the semi-circle, C_ε, contour is ½ E(x), E(x) being the steady state solution in Equations 39 and 42.

Form of the Solutions E(x,τ) and E(x)

The steady-state form of the E-system, along with its solution, is given in Table I. This solution was derived from Equations 39 to 42. The E-system itself, along with its time-varying solution, is summarized in Table II. The $E(x,\tau)$ solution was derived by following the steps in the previous

Table I. The Steady-State E-System and Solution

Governing Equations

$E''(x) - G^2E(x) = 0, \quad 0 < x < 1, \quad G^2 = \mu + \omega + b + \dfrac{a}{\mu + \omega}$
$E(0) = 1, \quad BE(1) + E'(1) = V$

Solution of the System

$E(x) = \dfrac{\left[B - V\cosh(G)\right]\sinh\left[(1-x)G\right] + \left[G + V\sinh(G)\right]\cosh\left[(1-x)G\right]}{B\sinh(G) + G\cosh(G)}$
where $G = +\left[\mu + \omega + b + \dfrac{a}{\mu + \omega}\right]^{1/2} > 0$

Table II. The Time-Varying E-System and Solution

Governing Equations

$E_{,\tau} - E_{,xx} + [b + \mu + \omega]\,E + a\exp[-(\mu + \omega)\tau] * E = 0$
$E = E(x,\tau), \quad 0 < x < 1, \quad \tau > 0$
$E(x,0) = 0, \quad 0 < x < 1$
$E(0,\tau) = 1, \quad \tau > 0$
$B\,E(1,\tau) + E_{,x}(1,\tau) = V, \quad \tau > 0$

Solution of the System

$E(x,\tau) = \dfrac{1}{2}\,E(x) + \dfrac{1}{\pi}\int_0^{\infty} M(x,\tau,\phi,V)\,d\phi$
$M(x,\tau,\phi,V) = \dfrac{1}{\phi}\left[L_1(x,\phi,V)\right]\sin\left[(\mu+\omega)\,\phi\tau\right] + + L_2(x,\phi,V)\,\cos\left[(\mu+\omega)\,\phi\tau\right]\Big]$
$L_1(x,\phi,V) = \dfrac{J_1(0,\phi,0)\;J_1(x,\phi,V) + J_2(0,\phi,0)\;J_2(x,\phi,V)}{J_1^2(0,\phi,0) + J_2^2(0,\phi,0)}$
$L_2(x,\phi,V) = \dfrac{J_1(0,\phi,0)\;J_2(x,\phi,V) - J_2(0,\phi,0)\;J_1(x,\phi,V)}{J_1^2(0,\phi,0) + J_2^2(0,\phi,0)}$

$J_1(x,\phi,V) = B\sinh[(1-x)\,H(\phi)]\cos[(1-x)\,F(\phi)] + H(\phi)\cosh[(1-x)\,H(\phi)]\cos[(1-x)\,F(\phi)] +$ $- F(\phi)\sinh[(1-x)\,H(\phi)]\sin[(1-x)\,F(\phi)] + V\sinh[xH(\phi)]\cos[xF(\phi)]$

$J_2(x,\phi,V) = B \cosh[(1-x)H(\phi)] \sin[(1-x)F(\phi)] + H(\phi) \sinh[(1-x)H(\phi)] \sin[(1-x)F(\phi)] + + F(\phi) \cosh[(1-x)H(\phi)] \cos[(1-x)F(\phi)] + V \cosh[xH(\phi)] \sin[xF(\phi)]$
$H(\phi) = \left[\frac{1}{2}\left\{\left[C^2(\phi) + D^2(\phi)\right]^{1/2} + C(\phi)\right\}\right]^{1/2}$
$F(\phi) = \left[\frac{1}{2}\left\{\left[C^2(\phi) + D^2(\phi)\right]^{1/2} - C(\phi)\right\}\right]^{1/2}$
$C(\phi) = \left[\mu + \omega + b + \frac{a}{\mu+\omega} \square \frac{1}{1+\phi^2}\right] > 0, \quad 0 \le \phi \le \infty$
$D(\phi) = \left[\mu + \omega - \frac{a}{\mu+\omega} \square \frac{1}{1+\phi^2}\right] \phi > 0, \quad \phi > 0; \quad D(0) = 0$

paragraph. For convenience sake, the η-variable of the previous paragraph was replaced by ϕ defined by:

$$\phi = \eta^2 \div 2(\mu + \omega), \qquad d\eta \div \eta = d\phi \div 2\phi . \qquad \text{(Eq. 49)}$$

Important Properties of E(x,τ) and E(x)

As $\tau \rightarrow \infty$, $E(x,\tau)$ should approach $E(x)$. This can best be seen by replacing $(\mu+\omega)\phi\tau$ in $M(x,\tau,\phi,V)$ in Table 2 by ξ. The differential $d\phi/\phi$ is replaced by $d\xi/\xi$, $L_1(x,\phi,V)$ approaches $E(x)$ as $\tau \rightarrow \infty$, and $L_2(x,\phi,V)$ approaches zero. Thus, we have:

$$E(x,\infty) = \frac{1}{2}E(x) + \frac{1}{\pi}E(x)\int_0^{\infty}\frac{\sin(\xi)}{\xi}\,d\xi = \frac{1}{2}E(x) + \frac{1}{\pi}E(x)\frac{\pi}{2} = E(x) . \qquad \text{(Eq. 50)}$$

The solution for $E(x,\tau)$ given in Table 2 is only meaningful if the integral of $M(x,\tau,\phi,V)$ converges for large and small values of ϕ. As ϕ approaches zero through positive values, one can show that $L_1(x,\phi,V)$ approaches a bounded function $B_1(x,V)$, while $L_2(x,\phi,V)$ approaches $B_2(x,V)\phi$, where $B_2(x,V)$ is also bounded. Thus, for small ϕ, we have:

$$M(x,\tau,\phi,V) \approx [B_1(x,V)\,(\mu+\omega)\tau\phi + B_2(x,V)\,\phi] \div \phi = \text{Bounded} . \qquad \text{(Eq. 51)}$$

For large values of ϕ, one can show that both $L_1(x,\phi,V)$ and $L_2(x,\phi,V)$ can be approximated by the following type of expression:

$$L_1(x,\phi,V) \text{ or } L_2(x,\phi,V) \rightarrow \left[B_3 \exp\left\{(x-1)m\sqrt{\phi}\right\} + B_4 \exp\left\{-xm\sqrt{\phi}\right\}\right] \div \sqrt{\phi} , \qquad \text{(Eq. 52)}$$

where B_3 and B_4 are bounded functions, and m is a positive constant. For $0 < x < 1$, Equation 52 shows that $M(x,\tau,\phi,V)$ decays exponentially as $\phi \rightarrow \infty$. For x = 1, Equation 52 shows that

$M(x,\tau,\phi,V)$ decays as $\phi^{-3/2}$. Thus, for $0 < x \leq 1$ and $\tau > 0$, the integral of $M(x,\tau,\phi,V)$ in the solution given in Table 2 is well-behaved.

In Table 1, we can see that $E(0) = 1$. Further, from Table 2, we can see that $L_1(0,\phi,V) = 1$ and $L_2(0,\phi,V) = 0$. Combining these results gives the following:

$$E(0,\tau) = \frac{1}{2}\,\square 1 + \frac{1}{\pi}\int_0^\infty \frac{\sin[(\mu+\omega)\phi\tau]}{\phi}\,d\phi \;=\; \frac{1}{2} + \frac{1}{\pi}\,\frac{\pi}{2} \;=\; 1, \quad \tau > 0\,. \qquad \text{(Eq. 53)}$$

Assuming that the solution $E(x,\tau)$ given in Table 2 satisfies the initial condition $E(x,0)= 0$, $0 < x < 1$, we obtain the following identity:

$$E(x) = -\,\frac{2}{\pi}\int_0^\infty \frac{L_2(x,\phi,V)}{\phi}\,d\phi \;=\; 0 < x < 1\,, \qquad \text{(Eq. 54)}$$

where more will be said about this identity later.

The quantities $E(x)$ and $E(x,\tau)$ satisfy the boundary condition at $x = 1$. From Table 1, we see that B $E(1)$ and $E'(1) = V$. Further, from Table 2, we see that

$$B\,L_1(1,\phi,V) + L_1'(1,\phi,V) = V\,, \qquad B\,L_2(1,\phi,V) + L_2'(1,\phi,V) = 0\,, \qquad \text{(Eq. 55)}$$

where the prime indicates the derivative with respect to x. Combining these results leads to the following:

$$B\,E(1,\tau) + E_{,x}(1,\tau) = \frac{V}{2} + \frac{V}{\pi}\int_0^\infty \frac{\sin[(\mu+\omega)\tau\phi}{\phi}\,d\phi = V, \quad \tau > 0\,. \qquad \text{(Eq. 56)}$$

Considering the functions in Table 2, one can show that

$$M_{,xx}(x,\tau,\phi,V) = C(\phi)\,M(x,\tau,\phi,V) + \frac{D(\phi)}{(\mu+\omega)\phi}\,M_{,\tau}(x,\tau,\phi,V)\,. \qquad \text{(Eq. 57)}$$

Further, the convolution integral in the governing equation for $E(x,\tau)$ can be written as:

$$\begin{aligned} a\,\exp[-(\mu+\omega)\tau] * E(x,\tau) \;=\; & \frac{a}{2(\mu+\omega)}\left[E(x) + \frac{2}{\pi}\int_0^\infty \frac{M(x,\tau,\phi,V)}{1+\phi^2}\,d\phi \;+\right. \\ & \left. -\,\frac{2}{\pi}\int_0^\infty \frac{M_{,\tau}(x,\tau,\phi,V)}{(\mu+\omega)(1+\phi^2)}\,d\phi\right] - \frac{a\,\exp[-(\mu+\omega)\tau]}{2(\mu+\omega)}\left[E(x) + \right. \\ & \left. -\,\frac{2}{\pi}\int_0^\infty \frac{\phi L_1(x,\phi,V) - L_2(x,\phi,V)}{\phi\left(1+\phi^2\right)}\,d\phi\right]\,. \end{aligned} \qquad \text{(Eq. 58)}$$

Using these results, we see that the specific E(x) and E(x,τ) in Tables 1 and 2, respectively, satisfy the governing equation for E(x,τ) if the following identity is satisfied:

$$E(x) = \frac{2}{\pi} \int_0^\infty \frac{\phi L_1(x,\phi,V) - L_2(x,\phi,V)}{\phi\left(1+\phi^2\right)}\, d\phi\ , \quad 0 \le x \le 1\ , \qquad \text{(Eq. 59)}$$

where the integral is defined at x = 0,1 such that E(0) = 1, and B E(1) + E'(1) = V.

Given the identities in Equations 54 and 59, we can derive the following set of identities:

$$\int_0^\infty \frac{L_1(x,\phi,V) + \phi\, L_2(x,\phi,V)}{1+\phi^2}\, d\phi = 0\ , \quad 0 < x < 1\ , \qquad \text{(Eq. 60)}$$

$$\int_0^\infty L_1(x,\phi,V)\, d\phi = 0\ , \quad 0 < x < 1\ . \qquad \text{(Eq. 61)}$$

These integrals converge for 0 < x < 1, and can be shown to be logically equivalent to Equations 54 and 59. For given sets of the system parameters defined in the "Governing Equations" section, we have numerically shown that Equations 60 and 61 are satisfied, which in turn, indicates that Equations 54 and 59 are satisfied, and that E(x) and E(x,τ) in Tables 1 and 2 are respectively the steady-state and time-varying solutions of the E-system of Equations 27 to 30.

THE EQUILIBRIUM SITE SOLUTION

The equilibrium site solution is defined by the parameters (f,ω) = (1,0). For these parameters, a = 0, b = B^2, and $G^2 = \mu + B^2$. The governing equation for E(x,t), Equation 27, reduces to

$$E_{,\tau} - E_{,xx} + G^2 E = 0\ . \qquad \text{(Eq. 62)}$$

Thus, the steady-state and time-varying solutions of Equations 62 and 28 to 30 have the same form as those given in Tables 1 and 2, except the functions on which M(x,τ,ϕ,V) depends are simpler. For example, C(ϕ) = G^2 and D(ϕ) = μϕ. These two functions simplify the partial derivative of M(x,τ,ϕ,V) in Equation 57:

$$M_{,xx}(x,\tau,\phi,V) = G^2\, M(x,\tau,\phi,V) + M_{,\tau}(x,\tau,\phi,V)\ . \qquad \text{(Eq. 63)}$$

Using Equation 63 and the fact that E"(x) = G^2 E(x), one can easily show that the solution in Table 2 satisfies Equation 62. Further, this reduced solution satisfies the boundary conditions in Equations 29 and 30, as well as the limit $E(x,\tau) \rightarrow E(x)$ as $\tau \rightarrow \infty$. The initial condition in Equation 28 leads to the identity given in Equation 54. Combining this identity with the differential equation E"(x) = G^2 E(x) leads to the identity in Equation 61. Conversely, the identity in Equation 61 leads to the identity in Equation 54.

A STEPWISE VARIABLE SOURCE AT THE SURFACE

The first step in replacing the unit source at the surface of the E-system by a stepwise variable source is to replace Equation 29 by

$$E(0,\tau;\ V,W) = W,\ \ \tau > 0\ , \qquad \text{(Eq. 64)}$$

where W is a nonzero constant. For convenience, the solution of Equations 27, 28, 64 and 30 is now denoted as E(x,t; V,W). The corresponding steady state solution is denoted by E(x; V,W). It can be shown that

$$E(x,\tau;\ V,W) = W\,E\left(x,\tau;\ \frac{V}{W},1\right)\ ,\quad E(x;\ V,W) = W\,E\left(x;\ \frac{V}{W},1\right)\ , \qquad \text{(Eq. 65)}$$

where $E(x,\tau;\ V/W,\ 1)$ and $E(x;\ V/W,\ 1)$ are the time-varying and steady-state solutions given respectively in Tables 2 and 1 when the V in these tables is replaced by V/W.

The next step in the process is to translate the source given in Equation 64 δ_a time units to the right (Figure 2) and to set V = 0 in Equation 30. The time translation can be accomplished through the use of Heaviside's step function, $H(\tau - \delta_a)$. The corresponding solution for Equations 27, 28, and 30 and the source strength (SS) given in Figure 2 is as follows:

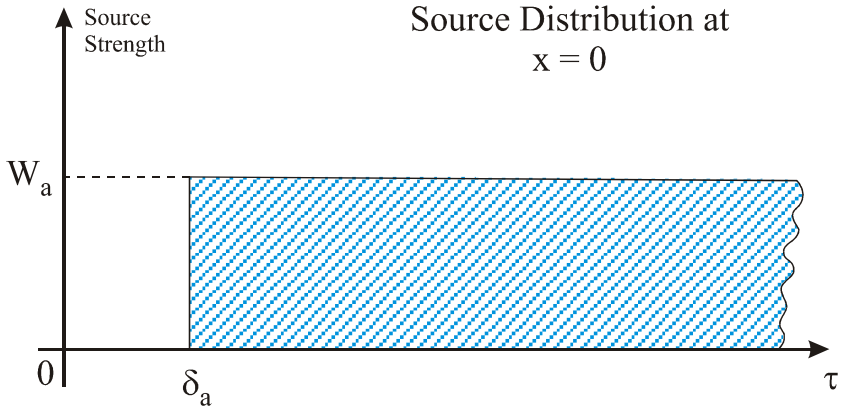

Fig. 2. Translation of the surface source δ_a time units to the right.

$$\begin{aligned} E(x,\tau;\ 0,\ W_a) &= H(\tau - \delta_a)\ E(x,\ \tau - \delta_a;\ 0,\ W_a) \\ &= W_a\ H(\tau - \delta_a)\ E(x,\ \tau - \delta_a;\ 0,1) \\ &= 0, \qquad \tau < \delta_a, \end{aligned}$$

$$= W_a\, E(x, \tau - \delta_a; 0,1), \quad \tau > \delta_a, \qquad \text{(Eq. 66)}$$

where the $M(x, \tau - \delta_a, \phi; 0,1)$ of Table 2 is given by

$$M(x,\ \tau - \delta_a,\ \phi;\ 0,\ 1) = \frac{1}{\phi}\ \Big[L_1(x,\ \phi;\ 0,\ 1)\ \sin[(\mu + \omega)\ (\tau - \delta_a)] + \\ + L_2(x,\ \phi;\ 0,\ 1)\ \cos[(\mu + \omega)\ (\tau - \delta_a)]\Big]\ . \qquad \text{(Eq. 67)}$$

The steady-state solution corresponding to $E(x,\tau;\ 0,\ W_a)$ is given by

$$E(x;0,W_a) = \frac{W_a\ B\ \sinh[(1\text{-}x)G] + W_a\ G\ \cosh[(1\text{-}x)G]}{B\ \sinh[G] + G\ \cosh[G]} \qquad \text{(Eq.68)}$$

The last step in the process is to take a finite number of source strengths of the type in Figure 2 and superimpose them in such a way as to form a stepwise variable source (Figure 3). Thus, Equation 29 is replaced by the following sum:

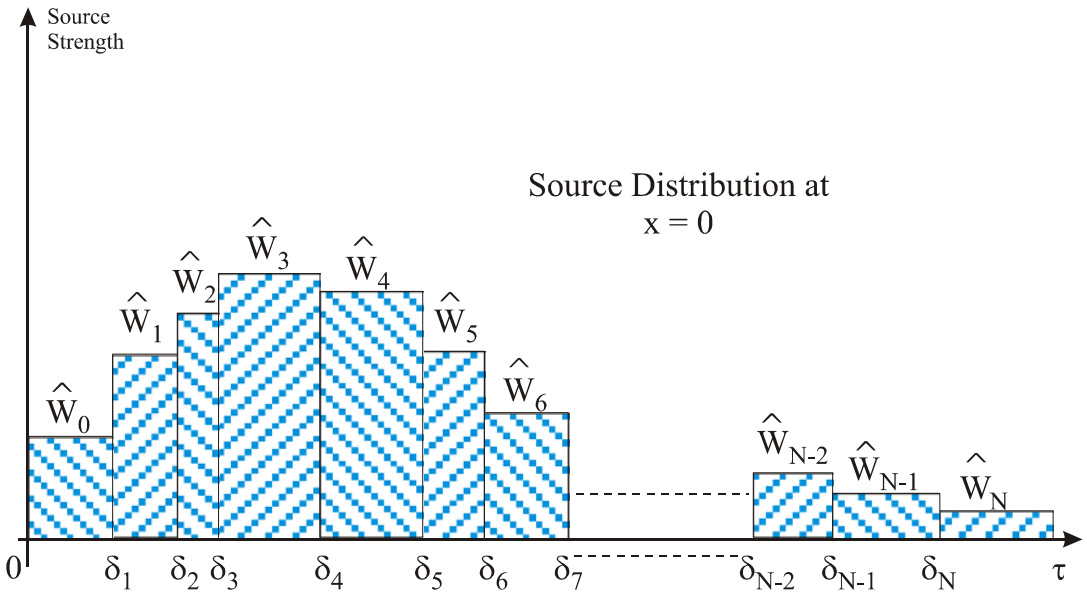

Fig. 3. A stepwise variable source strength at the surface, where $\hat{\mathbf{W}}_0 = \mathbf{W}_0$ and $\delta_0 = 0$.

$$E(0,\tau;\ V,\ SS) = \hat{W}_0 H(\tau) + \sum_{i=1}^{N} W_i\ H(\tau - \delta_i)\ , \qquad \text{(Eq. 69)}$$

where $\hat{W}_0 = W_0,\ \delta_0 = 0,\ W_i = \hat{W}_i - \hat{W}_{i-1}$ $(i = 1,2, \ldots, N)$. The solution of Equation 27, 28, 69 and 30 is given by

$$E(x,\tau;V,SS) = W_0\ E(x,\tau;V_0,1) + \sum_{i=1}^{\infty} W_i\ H(\tau - \delta_i)\ E(x,\tau - \delta_i;0,1)\ , \qquad \text{(Eq. 70)}$$

where $V_0 = V \div W_0$. The corresponding steady-state solution is given by

$$E(x;V,SS) = \frac{\hat{W}_N\left[B\ \sinh[(1\text{-}x)G] + G\ \cosh[(1\text{-}x)G]\right] + V\ \sinh(xG)}{B\ \sinh[G] + G\ \cosh[G]}\ , \qquad \text{(Eq. 71)}$$

where $V \leq 0$ and $\hat{W}_N \geq 0$. If $\hat{W}_N = 0$, then V must be zero to prevent unrealistic negative concentrations. If $\hat{W}_N > 0$, then realistic concentrations can occur for right combinations of the system parameters.

SUMMARY AND CONCLUSIONS

The objective of this paper was the derivation of an exact solution of a system for the assessment of the nonequilibrium sorption of radionuclides in a finite depth, vadose zone. There are eight key steps in the process of this derivation and subsequent analysis of the solution. These steps are briefly summarized in the following:

1. The **dimensional system** and its parameters are defined in Equations 1 to 11. Using the characteristic quantities in Equations 12 to 14, the corresponding **nondimensional system** for (C,S) is given by Equations 15 to 21, where C is the nondimensional concentration of the pollutant in solution, and S is the nondimensional concentration at the nonequilibrium sorption sites in the vadose zone.
2. The (C,S) system experiences three transformations. The first is the **elimination of S** in the C governing equations, Equations 22 to 25. The second is the **elimination of the advective term** in the C governing equation, Equation 26. This results in an E-system defined by Equations 26 to 30, where E is the modified, nondimensional pollutant concentration in solution. The third transformation is the **Laplace Transform** (Equation 31) of the E-system leading to an $\overline{E}$ – system defined by Equations 32 to 35.
3. The **$\overline{E}$-system is solved** by elementary techniques of ordinary differential equations giving the results in Equations 36 and 37. From this solution, the **Tauberian Theorems** allow information to be obtained about the initial and final values of the E-system solution, Equations 38 to 42.
4. The complexity of the $\overline{E}$ – system solution in Equation 37 leads to the use of the Bromwich integral in obtaining its **inverse Laplace Transform** (Equation 43) which results in the solution of the E-system. To apply the Bromwich integral, the **singular points** of $\overline{E}(x,s)$ in the complex s-plane have to be located (Equations 44 to 46), and the **path of integration** (Figure 1) has to be determined (Equations 47 to 49). The resultant **steady-state solution** E(x) and the **time-varying solution** $E(x,\tau)$ are respectively given in Tables 1 and 2.

5. Given these expressions in Tables 1 and 2, we were able to verify **several properties of the solutions**. Through a change of variable, the limit of $E(x,\tau)$ as $\tau \rightarrow \infty$ is indeed equal to the steady-state solution $E(x)$, Equation 50. The infinite integral in the solution $E(x,\tau)$ is well behaved over the entire interval $0 < \phi < \infty$, Equations 51 and 52. The boundary conditions in Equations 29 and 30 are satisfied by both $E(x,\tau)$ and $E(x)$, Equations 53, 55 and 56. The functions making up the solution $E(x,\tau)$ are such that the partial differential equation for $E(x,\tau)$ is satisfied (Equations 57 and 58). In the satisfaction of the initial condition in Equation 28 and the partial differential equation, **two identities** were obtained, Equations 54 and 59. These two identities are logically equivalent to **two other identities**, Equations 60 and 61. The authors numerically verified these last two identities for certain combinations of the system parameters.
6. Setting the parameters (f,ω) equal to $(1,0)$ in the expressions in Tables 1 and 2 results, respectively, in the steady-state and time-varying solutions for the **equilibrium site situation**. These new solutions satisfy the proper one-site, equilibrium-type equations (Equations 62 and 63), and lead to only **one identity**, Equation 54, and its logical equivalent Equation 61.
7. The E-system in Equations 27 to 30 can be extended to account for a **stepwise variable source** at the surface. The first step in this process is an improvement in notation (Equations 64 and 65), followed by a temporal translation in the source term (Figure 2, and Equations 66 to 68). Through the use of **Heaviside's step function**, the steady-state and time-varying solutions for a stepwise variable source are obtained (Figure 3, and Equations 69 to 71).

The **eighth step** in the solution process is the transformation of the various $E(x,\tau)$ results back to nondimensional concentrations $C(x,\tau)$ and dimensional concentrations $C^*(z,t)$, as well as determining the nonequilibrium sorbed phase concentrations, $S(x,\tau)$ and $S^*(z,t)$. Given (C,S), the quantities (C^*,S^*) can be determined from the transformations given in Equations 12 to 14. The concentration $C(x,\tau)$ can be obtained from $E(x,\tau)$ through the use of Equation 26. The sorbed concentration $S(x,\tau)$ can be determined from $E(x,\tau)$ by using Equations 22, 26, 58 and 59, and the formulas in Table 2:

$$S(x,\tau) = \frac{\omega(1-f)\,K_d\,C_0\,\exp[Bx]}{2(\mu+\omega)}\left[E(x) + \frac{2}{\pi}\int_0^\infty \left\{\frac{L_1(x,\phi,V) + \phi L_2(x,\phi,V)}{\phi(1+\phi^2)}\sin[(\mu+\omega)\phi\tau] + \right.\right.$$
$$\left.\left. + \frac{L_2(x,\phi,V) - \phi L_1(x,\phi,V)}{\phi(1+\phi^2)}\cos[(\mu+\omega)\phi\tau]\right\} d\phi\right]. \qquad \text{(Eq. 72)}$$

Replacing $[(\mu+\omega)\,\phi\tau]$ in the integral of Equation 72 by ξ, we can show that $d\phi/\phi$ is replaced by $d\xi/\xi$, and that $\phi \rightarrow 0$, $L_1 \rightarrow E(x)$, $L_2 \rightarrow 0$, as $\tau \rightarrow \infty$. Thus, the steady state value of $S(x,\tau)$ is given by

$$S(x,\infty) = \frac{\omega(1\text{-}f)\, K_d\, C_0}{\mu + \omega} \exp[Bx]\; E(x) = \frac{\omega(1\text{-}f)\, K_d\, C_0}{\mu + \omega}\, C(x,\infty)\,. \qquad \text{(Eq. 73)}$$

This result is consistent with the steady-state solution obtained from Equation 16. Further, if $\omega >> \mu$, then $\omega \div (\mu + \omega) \approx 1$, and Equation 11 is valid. That is to say, given the decay rate μ and given a sufficiently large sorption rate ω, then the nonequilibrium sorption sites tend to act as equilibrium sorption sites. Invoking the identity in Equation 59, we see that Equation 72 satisfies the initial condition $S(x,0) = 0$.

Several improvements or extensions of these solutions will be considered in the future:

- The four identities in Equations 54, 59, 60 and 61 will be further analyzed and verified for various combinations of the system parameters.
- The solutions will be efficiently programmed and comparative studies for the system parameters will be conducted.
- Stepwise variable boundary conditions at the water table will be introduced.
- A zero-order production term will be introduced into the governing equations for C* and S*.

DISCLAIMER

The U.S. Environmental Protection Agency through its Office of Research and Development funded and managed the research described here under U.S. EPA Contract No. 68-C-99-256 to Dynamac. It has been subjected to Agency review and approved for publication.

ACKNOWLEDGMENTS

The work was performed under U.S. EPA Contract No. 68-C-99-256 to Dynamac Corporation. The support of Dr. David Burden, the Project Officer for the Contract, is acknowledged.

REFERENCES

1. KNOX, R.C., D.A. SABATINI, and L.W. CANTER. "Subsurface Transport and Fate Processes." Lewis Publishers, Boca Raton, FL (1993).
2. THIBODEAUX, L.J. "Environmental Chemodynamics: Movement of Chemicals in Air, Water, and Soil." 2nd Edition. John Wiley & Sons, Inc. New York, NY (1996).
3. BROGAN, S.D. and R.M. GAILEY. "A method for estimating field-scale mass transfer rate parameters and assessing aquifer cleanup times." Ground Water. 33, 997-1009. (1995).
4. CHEN, J-S, R.L. DRAKE, Z. LIN and D. JEWETT. "Evaluation of Computer Models for Simulating Radionuclide Transport in the Unsaturated Zone." EPA Report under peer review. National Risk Management Laboratory, Subsurface Protection and Remediation Division, Ada, OK (2001).
5. ŠIMUNEK, J., K. HUANG, and M.TH. VAN GENUCHTEN. "The HYDRUS Code for Simulating the One-Dimensional Movement of Water, Heat, and Multiple Solutes in

Variably-Saturated Media." Research Report No. 144. U.S. Salinity Laboratory, USDA, ARS, Riverside, CA (1998).

6. VAN GENUCHTEN, M. TH., and R.J. WAGENET. "Two-site/two-region models for pesticide transport and degradation: theoretical development and analytical solutions." Soil Sci. Soc. Am. J. 53, 1303-1310. (1989).
7. TORIDE, N., F.J. LEIJ, AND M.T. VAN GENUCHTEN. "A comprehensive set of analytical solutions for nonequilibrium solute transport with first-order decay and zero-order production." Water Resour. Res. 29(7), 2167-2182 (1993).
8. LAND, N.S. "A Compilation of Nondimensional Numbers." NASA SP-274. Langley Research Center, NASA, Washington, DC (1972).
9. DEBNATH, L. "Integral Transforms and Their Applications." CRC Press, Boca Raton, FL (1995).
10. DUFFY, D.G. "Transform Methods for Solving Partial Differential Equations." CRC Press. Boca Raton, FL (1994).
11. OBERHETTINGER, F. and L. BADII. "Tables of Laplace Transforms." Springer-Verlag, New York, NY (1973).